The Characteristics, Swelling Ratio and Water Content Percentage of Chitosan-gelatin/limestone-based Carbonate Hydroxyapatite Composite Scaffold

by Devi Rianti

Submission date: 31-Mar-2023 11:57AM (UTC+0800)
Submission ID: 2051699285
File name: limestone-based_Carbonate_Hydroxyapatite_Composite_Scaffold.pdf (1,004.94K)
Word count: 6101
Character count: 31884

INTERNATIONAL JOURNAL OF INTEGRATED ENGINEERING VOL. 14 NO. 2 (2022) 13-23

IJIE

Journal homepage: http://penerbit.uthm.edu.my/ojs/index.php/ijie
ISSN : 2229-838X e-ISSN : 2600-7916

The International Journal of Integrated Engineering

The Characteristics, Swelling Ratio and Water Content Percentage of Chitosan-gelatin/limestone-based Carbonate Hydroxyapatite Composite Scaffold

Devi Rianti[1], Geo Fanny[1], Rania Vivian Nathania[1], Alqomariyah Eka Purnamasari[1], Rifayinqa Ruyani Putri[1], Helal Soekartono[1], Soebagio[1], Anita Yuliati [1*], Ardiyansyah Syahrom[2*]

[1]Department of Dental Material, Faculty of Dental Medicine,
Universitas Airlangga Mayjen. Prof. Dr. Moestopo, St. no. 47, Surabaya 60132, INDONESIA

[2]Medical Devices and Technology centre (MEDITEC), Institute of Human Centered and Engineering (iHumEn),
Universiti Teknologi Malaysia, 81310 UTM Skudai, Johor, MALAYSIA

*Corresponding Author

DOI: https://doi.org/10.30880/ijie.2022.14.02.003
Received 30 April 2021; Accepted 30 September 2021; Available online 02 June 2022

Abstract: The tissue engineering field has developed a scaffold that can be used to increase the bone regeneration process. Carbonate hydroxyapatite (CHA) is a well-known scaffold due to its human bones resembling components. The scaffold was synthesized from K, G, and limestone-based CHA using a freeze-drying method with K-G/CHA ratios (w/w) of 40:60, 30:70, 20:80, and 10:90. A Fourier transform infrared spectroscopy (FTIR), a scanning electron microscope-energy dispersive X-ray (SEM-EDX), and X-ray diffraction (XRD) were used to characterize the scaffold. The FTIR test showed some functional groups, such as hydroxyl, amide I, amide II, carbonate, and phosphate. The SEM-EDX test showed micropore (<50 um) and macropores (>50 um) structures as well as elements of C, N, O, Mg, Al, Si, P, and Ca. The XRD analysis obtained crystalline and amorphous particles. The water content percentage (WCP) values obtained were 61.29%, 64.30%, 67.71%, and 67.78%. The K-G/CHA composite scaffold with a ratio of 30:70 has ideal characteristics, a swelling ratio, and a water content percentage.

Keywords: Chitosan, gelatin, limestone-based carbonate hydroxyapatite, composite scaffold, medicine, swelling ratio

1. Introduction

Bone damage is one of the health problems that often occur in the field of dentistry. Bone destruction can be caused by periodontal disease, neoplastic disease, trauma, necrosis, or infection [1], [2]. Bones can be remodeled; however, severe fractures require surgical intervention to aid the healing process. In this case, a technique was employed to develop a 3D scaffold. The scaffold is combined with stem cells and growth factors to replace damaged tissue by supporting the differentiation of stem cells to new bone [3], [4]. The scaffold acts as a microenvironment that facilitates stem cells to attach. In addition, it may support cell proliferation that can induce bone formation. There are some requirements for an ideal scaffold such as biocompatible, biodegradable, osteoconductive, good porosity and it should have good mechanical properties [1], [5]. The scaffold's property is determined by the intrinsic properties and the combination of the chemical and physical properties of the material that constructs the scaffold [4].

The scaffold from chitosan, gelatin, and limestone-based Carbonate hydroxyapatite (CHA) was developed for application in the field of tissue engineering. Chitosan (K) is a polymer derived from chitin, which has a similar structure to glycosaminoglycan, which supports proliferation, the differentiation of osteoprogenitor cells, and bone formation [3], [6]. Chitosan can be applied clinically because of its good biocompatibility and biodegradation properties [7]. Gelatin

*Corresponding author: anita-y@fkg.unair.ac.id

(G) is a biopolymer resulting from the partial hydrolysis of collagen. Gelatin consists of arginine-glycine-aspartate (RGD) amino acid sequences, which support adhesion and cell migration, and it has good biocompatible and biodegradable properties [6]. Carbonate apatite is used in the field of bone tissue engineering because its content mostly resembles bone-building apatite compared to other calcium phosphates [8]. Carbonate apatite has osteoconductive and osteoinductive properties, and it can also stimulate osteogenesis with minimal immunological reactions [9–11].

The combination of chitosan and gelatin with carbonate apatite is expected to produce organic and inorganic compositions that resemble bone structures and produce good mechanical properties for implantation in bone defects [12]. The organic composition of bones consists of collagen and non-collagen components. The collagen component is represented by gelatin, while the non-collagen component is represented by chitosan [13]. In this study, we used CHA synthesized from Indonesian limestone, which is produced by Balai Besar Keramik Indonesia. Limestone contains calcium carbonate ($CaCO_3$), which can be used as a scaffold material in the form of apatite carbonate [14]. CHA is often used for scaffold materials because it has physicochemical properties, biocompatibility, and osteoconductivity is similar to inorganic components of bone [15]. The K-G/CHA composite scaffold was synthesized in four ratios (w/w), namely 40:60, 30:70, 20:80, and 10:90. These ratios are considered to be under the composition of the organic (22%) and inorganic (69%) components of bone with variations in the arithmetic series [12].

The K-G/CHA scaffold was synthesized by a freeze-drying method to obtain a porous scaffold [16]. The characteristics were analyzed using Fourier transform infrared spectroscopy (FTIR), a scanning electron microscope-energy dispersive X-ray (SEM-EDX), and X-ray diffraction (XRD). In addition, the swelling ratio and the water content percentage (WCP) analysis were also performed. The composition of the scaffold is important to produce the ideal scaffold [3]. The difference in the ratios of the scaffold component composition will affect the scaffold's characteristics. Thus, this study aimed to analyze the characteristics of various ratios of K-G/CHA scaffold and find the optimal ratios for the scaffold manufacture.

2. Materials and Methods

The materials used in this study were chitosan with a medium molecular weight (Sigma Aldrich 448877, USA), Bovine gelatin (Sigma Aldrich G9391, USA), CHA powder made from limestone produced by Balai Besar Keramik Indonesia (BBK Indonesia), natrium hydroxide (Biomedicine), acetic acid (Merck), aquadestilata (Duta Farma), and simulated body fluid (SBF Merck). The scaffold with a ratio of 40:60 (w/w) consists of 0.5 grams of chitosan, 0.5 grams of gelatin, and 1.5 grams of CHA. The scaffold with a ratio of 30:70 (w/w) consists of 0.375 grams of chitosan, 0.375 grams of gelatin, and 1.75 grams of CHA. The scaffold with a ratio of 20:80 (w/w) consists of 0.25 grams of chitosan, 0.25 grams of gelatin, and 2 grams of CHA. The scaffold with a ratio of 10:90 (w/w) consists of 0.125 grams of chitosan, 0.125 grams of gelatin, and 2.25 grams of CHA.

Gelatin was dissolved in 2 ml of 2% acetic acid by stirring at 50 °C. The CHA was mixed with 0.94 ml of distilled water and stirred until homogeneous. The diluted CHA was mixed with gelatin gel, and then chitosan powder was added to form a chitosan-gelatin gel and CHA. 0.5 ml of 0.1 M NaOH was added to neutralize the acid. The pH was checked to get the neutral pH (pH = 7), which was then added into the scaffold mold and frozen at -40 °C for 2 x 24 hours.

The functional groups of chitosan, gelatin, CHA, and K-G/CHA scaffold were analyzed using an FTIR (Thermo Scientific) with a wavelength of 400–4000 cm^{-1}. The resulting graph was then matched with the peak table. The XRD analysis was carried out using the X'Pert PRO PAN analytical tool. The monitor was rotated around the sample and set at an angle of 2θ to the incident flow. The results of this X-ray diffraction were imprinted on paper with a copper (Cu) radiation source with a nickel filter. An SEM-EDX analysis was obtained using EDAX-AMATEK, which was conducted at 100x and 500x magnification. In the SEM test, 10 pores at 100x magnification were randomly selected. The pore diameter was then measured using ImageJ software. The swelling analysis was carried out by weighing the initial weight of the scaffold (*Wi*), immersing the scaffold in distilled water for 24, 72, and 168 hours and then weighing it to get the final weight (*Wf*). The swelling value is calculated by the formula in Eq. 1.

$$Swelling = \frac{Wf-Wi}{Wi} \quad (1)$$

The WCP analysis was carried out by weighing the initial weight of the scaffold (*Wi*), immersing the scaffold in distilled water for 24, 72, and 168 hours and then weighing it to get the final weight (*Wf*). The WCP value is calculated by the formula in Eq. 2.

$$WCP = \frac{Wf-Wi}{Wf} \times 100\% \quad (2)$$

The data were analyzed using Saphiro-Wilk testing to see the normality of the data distribution and a Levene test to see the data homogeneity. If the data were normally distributed and homogeneous, it was continued with the one-way Anova test and Tukey's HSD. If the data were not normally distributed or homogeneous, they were analyzed using Kruskal Wallis and Mann Whitney. The values of $p < 0.05$ were considered statistically significant.

3. Results

3.1 Functional Group Analysis using FTIR

FTIR analysis was performed to analyze the presence of different functional groups for CHA BBK, chitosan, gelatin, and K-G/CHA scaffold, as shown in Fig. 1. It was found that CHA BBK has hydroxyl (-OH), carbonate (CO_3^{2-}), and phosphate (PO_4^{3-}) groups. The peak for the hydroxyl groups (-OH) bands at 3447.70 cm^{-1}, the carbonate groups (CO_3^{2-}) at 1424.90 cm^{-1}, and the phosphate groups (PO_4^{3-}) at 1086.78 cm^{-1}, 1026.73 cm^{-1}, and 961.64 cm^{-1} [17], [18]. Chitosan with a medium molecular weight has hydroxyl (-OH), C-H, amide I, amide II, and amine (C-N) functional groups. The peak for the hydroxyl groups (-OH) bands at 3293.93 cm^{-1}; the CH groups at 2873.88 cm^{-1}; the amide I groups at 1654.15 cm^{-1}, 1647.87 cm^{-1}, and 1637.14 cm^{-1}; the amide II groups at 1508.13 cm^{-1} and 1458.38 cm^{-1}; and the amine groups at 1149.20 cm^{-1} and 1023.57 cm^{-1} [17], [18].

In gelatin, there are hydroxyl groups (-OH), amide I, carboxylate (-COO), and amine functional groups. The peak for the hydroxyl groups (-OH) bands at 3271.25 cm^{-1} and 2935.17 cm^{-1}, the amide I groups at 1633.37 cm^{-1}, the carboxylate (-COO) groups at 1234.4 cm^{-1}, and the amine groups at 1077.98 cm^{-1} [17], [18]. The K-G/CHA scaffold with four different ratios showed the presence of the same functional groups, namely the hydroxyl (-OH) groups with peaks at around 3292.09–3447.43 cm^{-1}, the amide I groups at around 1654.37–1636.79 cm^{-1}, the amide II groups at around 1483.47–1482.31 cm^{-1}, the carbonate groups at around 1423.18–1420.81 cm^{-1}, and the phosphate groups at around 1086.88–961.29 cm^{-1}.

3.2 X-ray Diffraction (XRD) Analysis

XRD was performed to analyze the structural properties, as shown in Fig. 2. CHA BBK has clear peak patterns, indicating that it has a crystalline form. It showed a similar pattern with synthetic hydroxyapatite. The XRD patterns of chitosan showed that there are were two high peaks with a wide and sloping distance, which indicates that chitosan has a semi-crystalline form. The gelatin sample showed a sloping peak, indicating that gelatin has an amorphous form. The pattern of the K-G/CHA scaffold samples with 40:60 (w/w), 30:70 (w/w), 20:80 (w/w), and 10:90 (w/w) ratios were firm and sloping peaks. This pattern indicated that the scaffold form is a combination of being crystalline and amorphous.

3.3 Scanning Electron Microscopy-energy Dispersive X-ray (SEM-EDX) Analysis

Based on the SEM analysis, the K-G/CHA scaffold with ratios of 40:60 (w/w), 30:70 (w/w), 20:80 (w/w), and 10:90 (w/w) has pore sizes range of 30.42-282.7 μm, 40.59-153.8 μm, 43.71-441.0 μm, and 44.10-145.2 μm, respectively (Table 2).

Table 2 - The Pore size of various K-G/CHA scaffold ratios

No	K-G/CHA scaffold ratios	Pore size range	Mean	SD
1	40:60	30,42-282,7 μm	108,72 μm	75.27
2	30:70	40,59-153,8 μm	69,405 μm	35.32
3	20:80	43,71-441 μm	127,69 μm	118.67
4	10:90	44,10-145,2 μm	109,75 μm	37.77

Based on the results of the EDX analysis shown in Fig. 3–7, CHA BBK contained six elements, namely O, Mg, Al, Si, P, and Ca. Moreover, there were eight elements contained in the K-G/CHA scaffold, namely C, N, O, Mg, Al, Si, P, and Ca. The Ca/P ratio was calculated using the atomic percentages of Ca and P, which were obtained from the EDX analysis. It was found that CHA BBK has a Ca/P ratio of 1.81. After the CHA BKK was combined with chitosan and gelatin to form the K-G/CHA scaffold, it was found that the ratio of 40:60 (w / w) had the smallest Ca/P ratio (1.65) and the ratio of 20:80 (w/ w) had the largest Ca/P ratio (1.99) (Table 3).

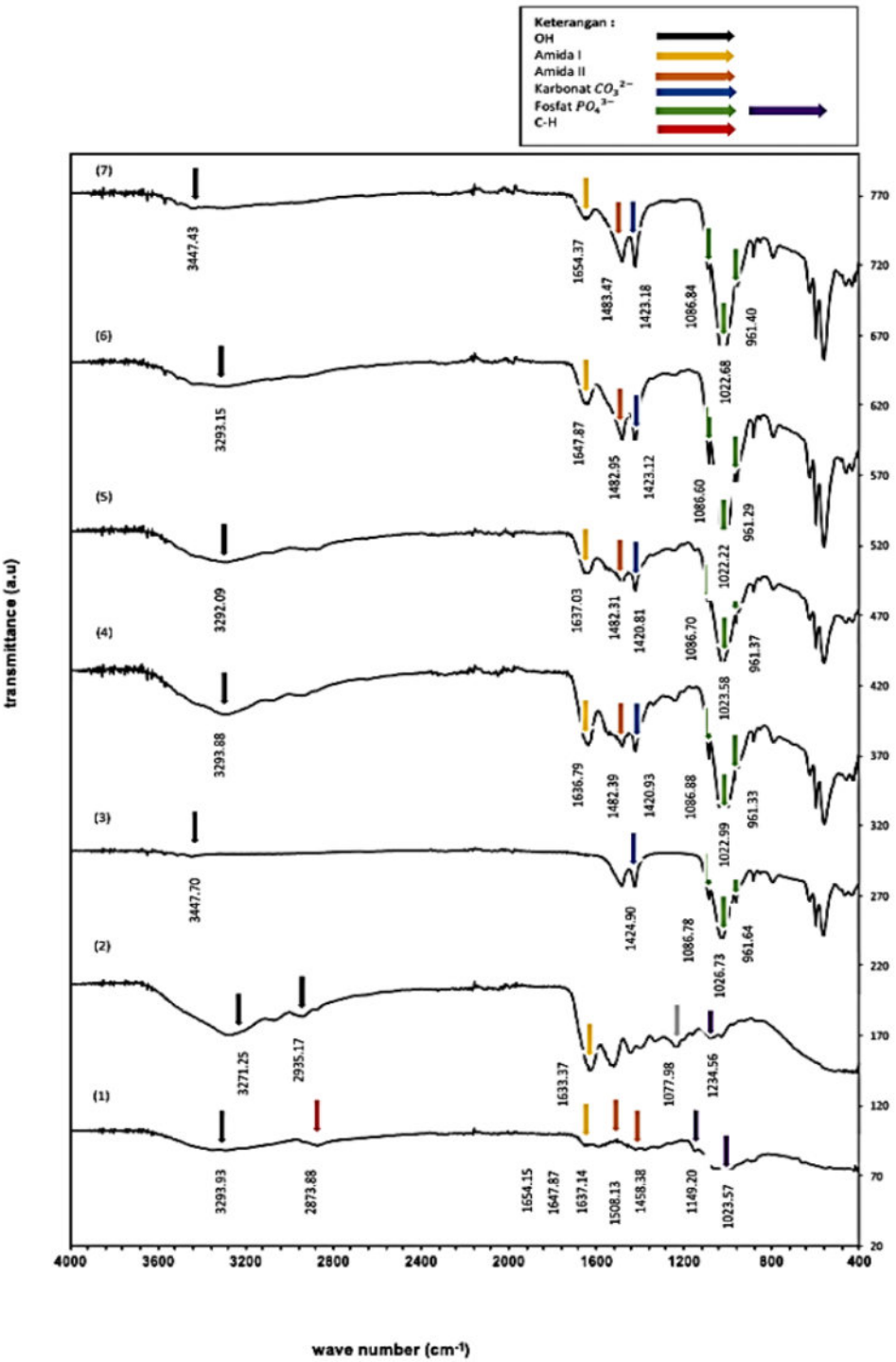

Fig. 1 - The FTIR pattern of chitosan (1), gelatin (2), and CHA BBK (3) K-G/CHA scaffold with ratios of 40:60 (4), 30:70 (5), 20:80 (6), and 10:90 (7)

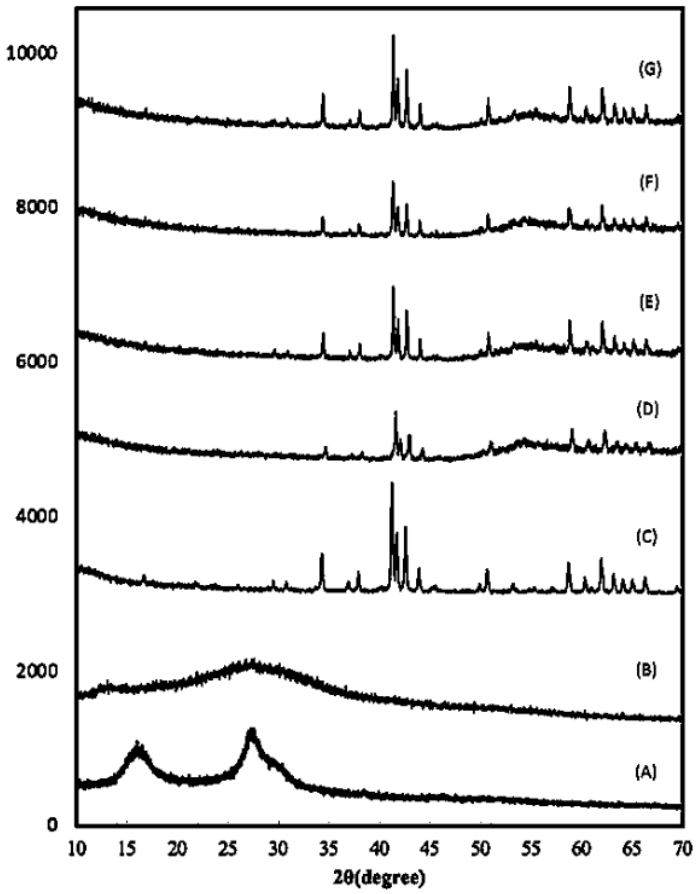

Fig. 2 - X-ray diffraction pattern of chitosan (A), gelatin (B), CHA BBK (C), and K-G/CHA scaffold with ratios of 40:60 (D), 30:70 (E), 20:80 (F), and 10:90 (G)

Table 3 - Energy dispersive X-ray (EDX) analysis at 100x magnification

Sample	Ca (At %)	P (At %)	Ca/P ratio
CHA BBK	26.43	14.59	1.81
K-G/CHA 40:60	15.92	09.65	1.65
K-G/CHA 30:70	18.02	10.66	1.69
K-G/CHA 20:80	20.44	10.27	1.99
K-G/CHA 10:90	21.41	11.57	1.85

3.4 Swelling Ratio and Water Content Percentage (WCP) Analysis

Figures 8 and 9 showed that the less CHA composition, the greater the mean value of the WCP. On the other hand, the duration of immersion affects the swelling ratio, the longer the immersion duration, the higher the swelling ratio. The results of the normality test using the Saphiro-Wilk test and the homogeneity using the Levene test showed that the swelling data were normally distributed and homogeneous ($p > 0.05$). The statistical tests using the one-way ANOVA showed that there is a significant difference ($p = 0.000$) between the K-G/CHA scaffold ratio and the swelling ratio value, indicating that the higher the CHA composition, the lower the swelling ratio value. Using Tukey's HSD statistical test, a significant difference was found between the K-G/CHA scaffold ratios of 10:90, 30:70, and 40:60 also between the ratios of 20:80 and 40:60 ($p < 0.05$). There was a significant difference between 24, 72, and 168 hours of immersion ($p < 0.05$).

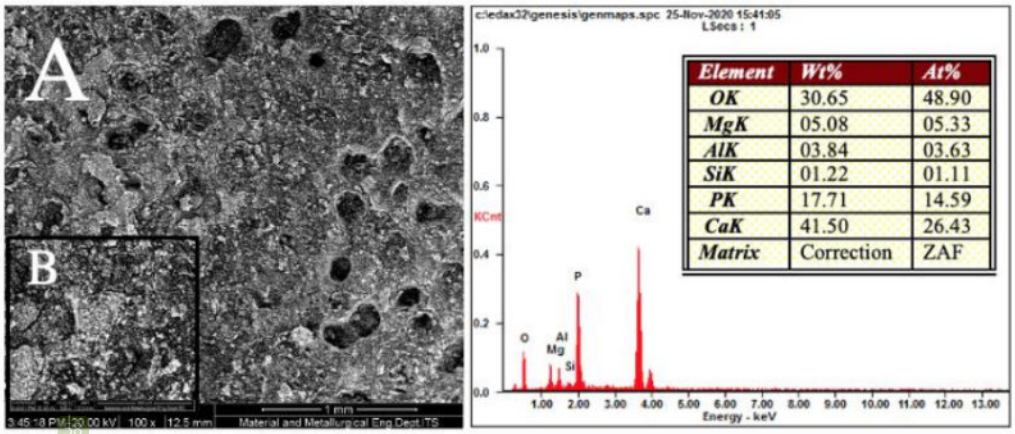

Fig. 3 - The SEM-EDX analysis shows the surface morphology and composition of CHA BBK at a magnification of 100x (A) and 500x (B)

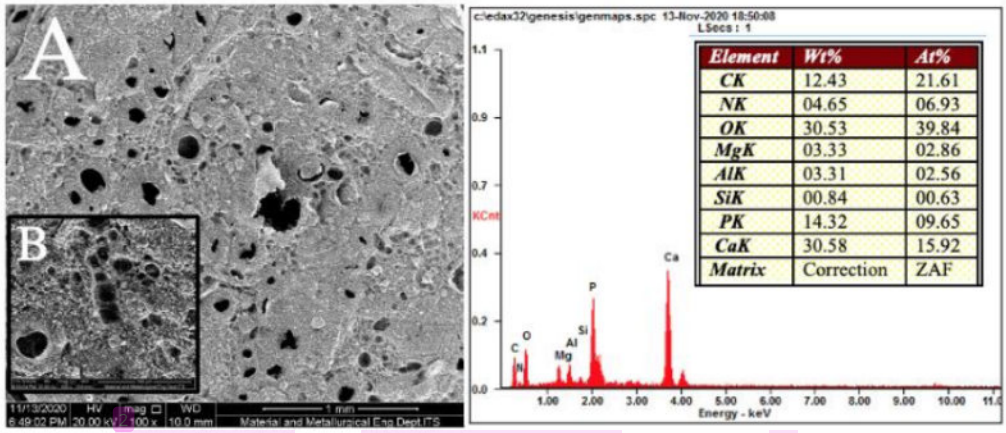

Fig. 4 - The SEM-EDX analysis shows the surface morphology and composition of the K-G/CHA40:60 (w/w) scaffold at 100x (A) and 500x (B) magnification

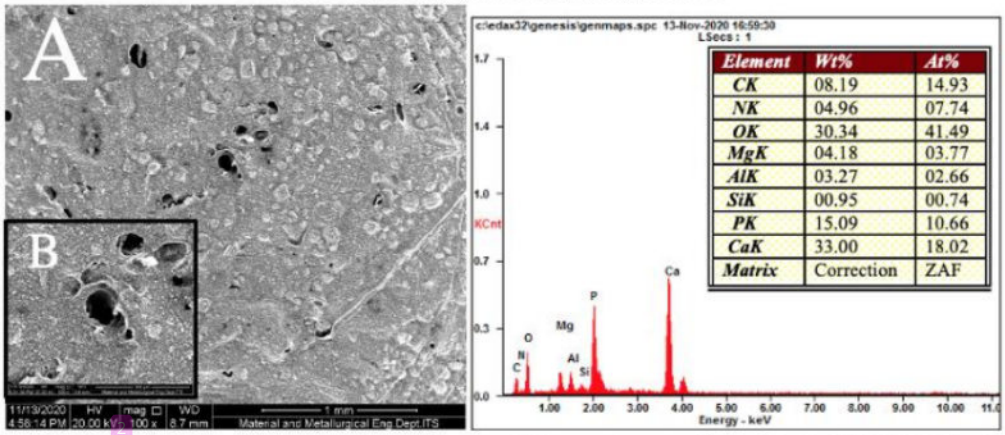

Fig. 5 - The SEM-EDX analysis shows the surface morphology and composition of the K-G/CHA30:70 (w/w) scaffold at 100x (A) and 500x (B) magnification

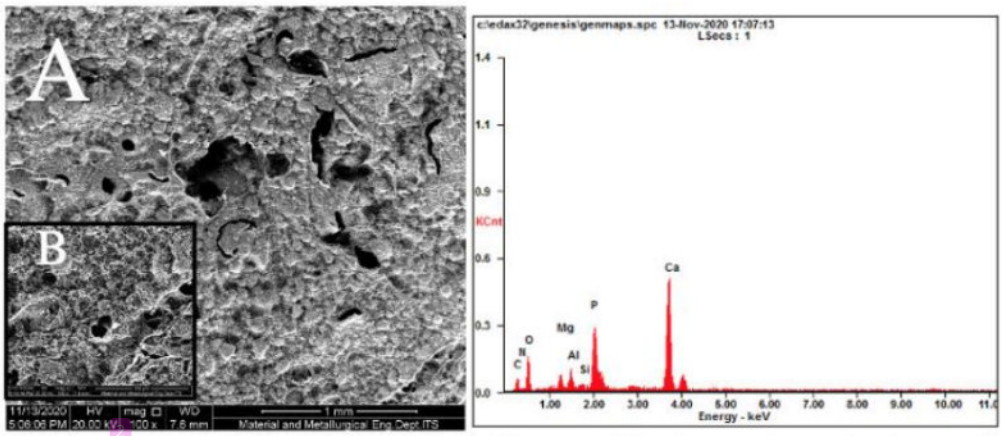

Fig. 6 - The SEM-EDX analysis shows the surface morphology and composition of the K-G/CHA20:80 (w/w) scaffold at 100x (A) and 500x (B) magnification

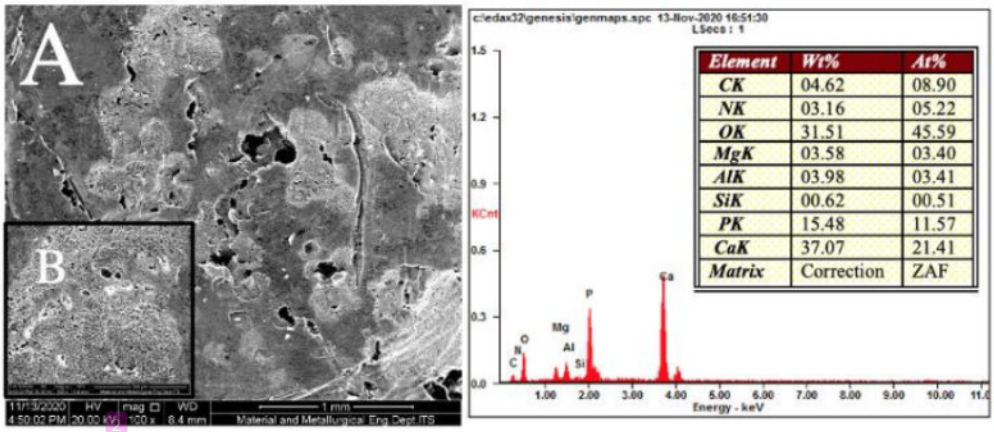

Element	Wt%	At%
CK	04.62	08.90
NK	03.16	05.22
OK	31.51	45.59
MgK	03.58	03.40
AlK	03.98	03.41
SiK	00.62	00.51
PK	15.48	11.57
CaK	37.07	21.41
Matrix	Correction	ZAF

Fig. 7 - The SEM-EDX analysis shows the surface morphology and composition of the K-G/CHA10:90 (w/w) scaffold at 100x (A) and 500x (B) magnification

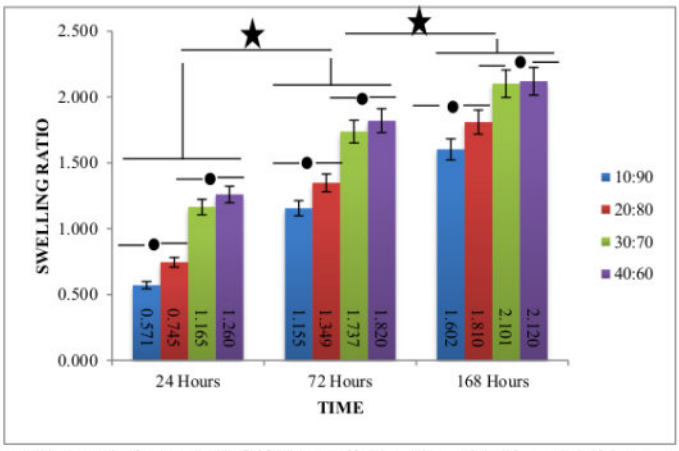

Fig. 8 - The swelling ratio for each K-G/CHA scaffold ratio at 24, 72, and 168 hours of immersion

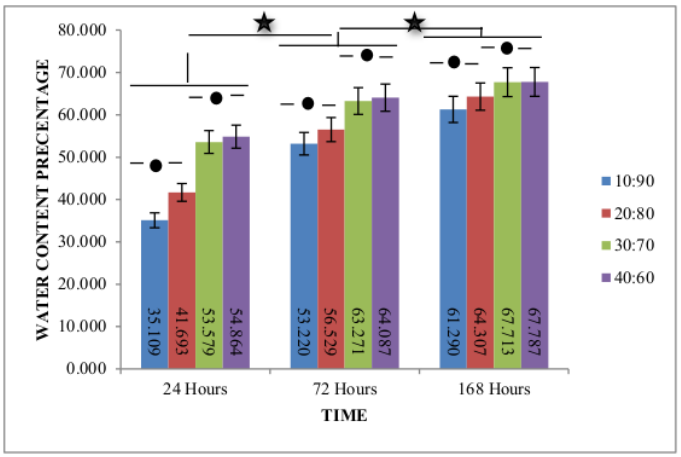

Fig. 9 - The water content percentage for each K-G/CHA scaffold ratio at 24, 72, and 168 hours of immersion

Figures 8 and 9 show that the less the CHA composition, the greater the swelling and WCP mean values. When immersed for 24, 72, and 168 hours, it showed that the longer the immersion duration, the more the swelling ratio and WCP were increased. The Saphiro-Wilk and Levene tests showed that the swelling data were normally distributed and homogeneous ($p > 0.05$), while the WCP data were not normally distributed ($p < 0.05$) but were homogeneous ($p > 0.05$). The one-way Anova and Kruskal Wallis tests showed that there were significant differences between each K-G/CHA scaffold ratio to swelling ratio ($p = 0{,}000$), and the WCP ($p = 0{,}001$) indicated that the higher the CHA composition, the lower the swelling ratio and WCP values. Furthermore, to determine which ratio had a significant difference, the Tukey HSD test for swelling and the Mann Whitney test for the WCP were obtained. There were significant differences in the swelling ratio and the WCP on the K-G/CHA scaffold ratios of 10:90, 30:70, and 40:60 and between the ratios of 20:80, 30:70, and 40:80. There was a significant difference between 24, 72, and 168 hours of immersion ($p < 0.05$).

4. Discussion

The spectra and FTIR peak values of the K-G/CHA scaffolds can be seen in Fig. 2, which shows the presence of hydroxyl groups (OH-) and indicates the involvement of the three biomaterials in the scaffold formation. The hydroxyl group (-OH) comes from the presence of hydrated inorganic compounds. The presence of the carbonate and phosphate groups were found in the CHA. The carbonate group is a marker of carbonate substitution in the apatite structure, while the phosphate group is a marker for the presence of minerals that support bone growth. A previous study showed the presence of hydroxyl, carbonate, and phosphate functional groups in carbonate apatite synthesized by the precipitation method [19]. These three groups were identified in the K-G/CHA scaffold, which indicates carbonate apatite involvement in the scaffold.

The presence of amide I, carboxylate, and amine groups could be identified in type B gelatin from bovine. Gelatin contains Arg-Gly-Asp (RGD) sequences, which are composed of several amino acids. Amino acids are organic compounds that contain amine and carboxylic functional groups, which can be identified from a FTIR band. RGD sequences support bone cell adhesion and migration [6], [20]. The involvement of gelatin in the K-G/CHA scaffold is characterized by the presence of an amide group I. Chitosan with a medium molecular weight has C-H, amide I, amide II, and amine groups. The C-H group is a marker of the polysaccharide structure of chitosan, while the hydroxyl and amine groups are reactive functional groups that increase the bonds between the biomaterials [20], [21]. Hydroxyl groups, C-H, amide I, amide II, and amine groups were found in commercial chitosan (Sigma-Aldrich) [22], [23]. The involvement of chitosan in K-G/CHA is characterized by the presence of amide groups I and amide II.

Amide I and amide II contain C-N groups that show the cross-linking between gelatin and chitosan, which forms the interconnectivity of the scaffold. The chitosan-gelatin complex shows structural similarities with glycosaminoglycans and collagen of an extracellular matrix. In addition, cross-linking between chitosan and gelatin improves the mechanical properties and pore interconnectivity of the scaffold [24]. An XRD analysis was carried out to determine the shape of the sample's particles (Fig. 3). The carbonate apatite obtained a clear pattern at each peak and high intensity, indicating that it has a crystalline form. The peak pattern of carbonate apatite is similar to synthetic hydroxyapatite (Sigma-Aldrich) because the carbonate apatite used in this study (CHA BBK) is carbonate ions (calcium carbonate and magnesium carbonate to form CHA) added to hydroxyapatite. The addition of carbonate ions causes changes in the crystal morphology and decreases the crystallinity, which thereby increases the solubility of the materials [25].

The pattern of the XRD analysis on the chitosan sample showed a wide diffraction peak at 2θ=10.01° and 20.05° then the intensity decreased (Fig. 2). This pattern indicates a semi-crystalline characteristic, and it has a dominant amorphous structure. The XRD pattern on the gelatin sample showed sloping diffraction between the peaks of 19.95°–41.66°, which indicated the presence of an amorphous form (Fig. 3). The results of the study were due to the sloping diffraction because of signals from the amorphous polysaccharides [26]. Former study also argued that there was a dominant amorphous structure in chitosan and the gelatin samples [6]. The XRD analysis was carried out on the K-G/CHA scaffold with ratios of 40:60 (w/w), 30:70 (w/w), 20:80 (w/w), and 10:90 (w/w) shows a firm peak pattern with high intensity and gentle peaks (Fig. 2). This shows that the form of the particle structure of the K-G/CHA scaffold is a crystalline and amorphous combination due to the presence of carbonate apatite, chitosan, and gelatin on the scaffold. The crystalline form is obtained from apatite carbonate, while the amorphous form is obtained from chitosan and gelatin.

The results of the SEM-EDX analysis can be seen in Fig. 3–7. A freeze-drying technique produces a scaffold morphology with a porosity of up to 90% [16]. The data from our unpublished data showed that the K-G/CHA scaffold with four ratios has a porosity of around 57.40%. The lower the polymer concentration, the higher the porosity percentage. This is because, at low polymer concentrations, the viscosity of the gel will be lower and contain more water. During the freeze-drying process, the water contained will sublimate and produce a larger pore size and porosity. The results of this study are following other studies that stated an increase in the percentage of porosity due to the reduction in the concentration of alginate as a polymer [27]. The porosity, which is suitable for application in the tissue engineering field, is around 50-90%. The scaffold with this porosity percentage shows the ideal pore interconnectivity for cell tissue growth, and it supports the osteoinduction properties [6], [28]. Based on these results, it can be concluded that it is feasible to apply the K-G/CHA scaffold with four different ratios in the field of tissue engineering due to the supports of cell growth.

A scaffold as a bone substitute material must have a micropore and macropore structure. Micropores (<50 µm in diameter) support osteoblast adhesion and growth factors, while macropores (>50 µm in diameter) support bone growth and bone tissue vascularization [29], [30]. The pores required for bone mineralization are at least 100 µm to provide a conducive environment for cell survival and bone remodeling. Moreover, micropores are required for bone maturation and formation [31]. Based on Table 2, it shows that there are micropore and macropore structures in the K-G/CHA scaffolds with a ratio of 40:60 (w/w), 30:70 (w/w), 20:80 (w/w), and 10:90 (w/w). According to previous research data, the pore size of around 50–300 µm allows for adhesion, growth, and migration of vascular tissue [15].

An EDX analysis is used to identify and measure the percentage of elemental composition contained in the scaffold [32]. CHA BBK consists of oxygen (O), magnesium (Mg), aluminum (Al), silicon (Si), phosphorus (P), and calcium (Ca). The K-G/CHA scaffolds with four different ratios consist of the same elements as CHA BKK, namely carbon (C), nitrogen (N), oxygen (O), magnesium (Mg), aluminum (Al), silicon (Si), phosphorus (P), and calcium (Ca). These results indicated the involvement of apatite carbonate in the K-G/CHA scaffold (Fig. 4–7). CHA on the scaffold plays a role in attracting calcium and phosphorus ions to induce osteogenesis [32]. The Ca/P ratio of adult bone tissue is 1.71, and hydroxyapatite is 1.67. It is considered to be the most effective ratio for bone regeneration [33], [34].

The atomic ratio of Ca/P in Table 3 was supported by other studies, which stated that carbonate apatite synthesized from calcium sulfate hemihydrate and calcium hydroxide obtained a Ca/P ratio of around 1.53–2.01 [35]. Based on the results of the study, the four different ratios meet the criteria for use in tissue engineering. A K-G/CHA scaffold with a ratio of 30:70 (w/ w) is considered the most optimal because it has a Ca/P ratio that is almost the same as the Ca/P ratio of hydroxyapatite by stoichiometry and bone Ca/P. After the swelling ratio and WCP analysis were conducted, it showed that the higher the CHA composition, the lower the swelling ratio and WCP values. This is probably because it used CHA derived from hydroxyapatite, which is a carbonate group substitution. Hydroxyapatite has the same chemical structure as nano-hydroxyapatite [$Ca_{10}(PO_4)_6(OH)_2$]. The CHA components affect the cross-linking between CHA with chitosan and gelatin. Nano-hydroxyapatite forms cross-links between chains and reduces the hydrophilicity of gelatin by binding calcium and phosphate to hydrophilic groups—COOH or NH2. Some NH2 from chitosan binds to calcium groups, and then the OH groups cannot form hydrogen bonds, which thereby reduces the swelling ratio of the scaffold [36], [37].

The swelling and water absorption is are also affected by the duration of immersion, where the values of the swelling ratio and WCP increase to the highest peak at 168 hours of immersion. The value of the swelling ratio and WCP is are also affected by the hydrophilic scaffold materials, namely chitosan, gelatin, and carbonate apatite [38–40]. At a high swelling ratio and high WCP values, the liquid is easier to penetrate the scaffold so that the scaffold degrades faster [41]. The scaffold was developed to be an efficient protein transport, which is not only in large quantities but also gradually [42]. The ability of the swelling affects the hydrophilic properties of the scaffold is important for the scaffold to carry calcium and phosphate ions into the scaffold for new tissue formation [43]. The values of the swelling ratio and WCP affects the hydrolysis and the physical properties, which are good for the scaffold in nutrient transport, which is important for the bone regeneration process [44]. Based on previous studies, it is stated that the swelling ratio and WCP can affect the hydrophilic properties of a scaffold. The higher the value of the swelling ratio and WCP, the better the hydrophilic properties. In our study, the highest swelling ratio value was obtained from a K-G/CHA scaffold with a ratio of 40:60, namely 2.120 ± 0.11, and the highest WCP value of 67.78% ± 1.21 was also obtained from the K-G/CHA scaffold with a ratio of 40:60. The K-G/CHA scaffold ratios of 40:60 and 30:70 have no significant difference; therefore, the two K-G/CHA scaffold ratios have the same properties. The K-G/CHA scaffold with a ratio of 30:70 was considered suitable because it is similar to the components of the bone extracellular matrix.

5. Conclusion

A K-G/CHA scaffold with four different ratios, 40:60 (w/ w), 30:70 (w/ w), 20:80 (w/w), and 10:90 (w/w) has the appropriate functional groups, the crystal and amorphous particles form, micropore, and macropore structures, and the same elemental content. A K-G/CHA scaffold with a ratio of 30:70 (w/w) has the most ideal ratio (1.69). A K-G/CHA scaffold with a ratio of 30:70 has an ideal value of the swelling ratio (2.10 ± 0.11) and WCP (67.71% ± 0.56).

References

[1] Ghassemi, T., Shahroodi, A., Ebrahimzadeh, M. H., Mousavian, A., Movaffagh, J., & Moradi, A. (2018). Current concepts in scaffolding for bone tissue engineering. Archives of Bone and Joint Surgery, 6(2), 90–99.

[2] Funda, G., Taschieri, S., Bruno, G. A., Grecchi, E., Paolo, S., Girolamo, D., & Fabbro, M. D. (2020). Nanotechnology scaffolds for alveolar bone regeneration. Materials (Basel), 13(1), 1–20.

[3] Oryan, A., & Sahvieh, S. (2017). Effectiveness of chitosan scaffold in skin, bone and cartilage healing. International Journal of Biology Macromolecule, 104, 1003–1011.

[4] Willerth, S. M., & Sakiyama-Elbert S. E. (2019). Combining stem cells and biomaterial scaffolds for constructing tissues and cell delivery. StemJournal, 1(1), 1–25.

[5] Black, C. R. M., Goriainov, V., Gibbs, D., Kanczler, J., Tare, R. S., & Oreffo, R. O. C. (2015). Bone tissue engineering. Current Molecular Biology Report, 1(3), 132–140.

[6] Maji, K., Dasgupta, S., Pramanik, K., & Bissoyi, A. (2016). Preparation and evaluation of gelatin-chitosan-nanobioglass 3D porous scaffold for bone tissue engineering. International Journal of Biomaterials, 1–15.

[7] Wahid, F., Khan, T., Hussain, Z., & Ullah, H. (2018). Nanocomposite scaffolds for tissue engineering; Properties, preparation, and applications. Applications of Nanocomposite Materials in Drug Delivery, 701–735.

[8] Ishikawa, K., Miyamoto, Y., Tsuchiya, A., Hayashi, K., Tsuru, K., & Ohe, G. (2018). Physical and histological comparison of hydroxyapatite, carbonate apatite, and β-tricalcium phosphate bone substitutes. Materials (Basel), 11(10), 1–12.

[9] Rahyussalim, A. J., Supriadi, S., Marsetio, A. F., Pribadi, P. M., & Suharno, B. (2019). The potential of carbonate apatite as an alternative bone substitute material. Medical Journal of Indonesia, 28(1), 92–97.

[10] Setiawatie, E. M., Prihartini, W., Ryan, M., & Rubianto, M. (2019). Carbonate hydroxyapatite-hyaluronic acid as bone healing accelerator: In-vitro and in-vivo studies on the alveolar bone of Wistar rats. Journal of International Dental and Medical Research, 1294, 1280–1286

[11] Prahasanti, C., Subrata, L. H., Saskianti, T., Suardita, K., & Ernawati, D. S. (2019). Combined hydroxyapatite scaffold and stem cell from human exfoliated deciduous teeth modulating alveolar bone regeneration via regulating receptor activator of nuclear factor-Kb and osteoprotegrin system. Iranian Journal of Medical Sciences, 44(5), 415–421

[12] Chocholata, P., Kulda, V., & Babuska, V. (2019). Fabrication of scaffolds for bone-tissue regeneration. Materials (Basel), 12(4), 1–25.

[13] Fadhlallah, P. M. E., Yuliati, A., Soesilawati, P., & Pitaloka, P. (2018). Biodegradation and compressive strength test of scaffold with different ratio as bone tissue engineering biomaterial. Journal of International Dental and Medical Research, 11(2), 587–590.

[14] Noviyanti, N., Jasruddin, J., & Sujiono, E. H. (2015). Karakterisasi kalsium karbonat ($Ca(CO_3)$) dari batu kapur kelurahan Tellu Limpoe kecamatan Suppa. Jurnal Sains dan Pendidikan Fisika, 11(2), 169–172.

[15] Salim. S., & Ariani, M. D. (2015). In vitro and in vivo evaluation of carbonate apatite-collagen scaffolds with some cytokines for bone tissue engineering. The Journal of the Indian Prosthodontic Society, 15(4), 349–355.

[16] Fereshteh, Z. (2018). Freeze-drying technologies for 3D scaffold engineering. In functional 3D tissue engineering scaffolds. Materials, Technologies, and Applications, 151–174.

[17] Stuart, B. H. (2004). Infrared spectroscopy: fundamentals and applications. Hoboken, New Jersey: John Wiley & Sons, Ltd.

[18] Nikolicc, G. (2012). Fourier transforms - New analytical approaches and FTIR strategies. London, United Kingdom: InTechOpen.

[19] Bang, L. T., Ramesh, S., Purbolaksono J., Long, B. D., Chandran, H., & Ramesh S., (2015). Development of a bone substitute material based on alpha-tricalcium phosphate scaffold coated with carbonate apatite/poly-epsilon-caprolactone. Biomedical Materials, 10(4), 1–13.

[20] Babu, R. J., Annaji, M., Alsaqr, A., & Arnold, R. D. (2019). Animal-based materials in the formulation of nanocarriers for anticancer therapeutics. In polymeric nanoparticles as a promising tool for anti-cancer therapeutics. 319–341.

[21] El-Meliegy, E., Abu-Elsaad, N. I., El-Kady, A. M., & Ibrahim, M. A. (2018). Improvement of physico-chemical properties of dextran-chitosan composite scaffolds by addition of nano-hydroxyapatite. Scientific Reports, 8(1), 1–10.

[22] Varan, N. (2017). The use of titration technique and FTIR bands to determine the deacetylation degree of chitosan samples. Journal of Textile Science and Engineering, 7(1), 1–4.
[23] Zuniga, Z. A., Garcia, M. J., & Cervantes, G. E. (2016) Removal of congo red from the aqueous phase by chitin and chitosan from waste shrimp. Desalination of Water Treatment, 57(31), 14674–14685.
[24] Afewerki, S., Sheikhi, A., Kannan, S., Ahadian, S., & Khademhosseini A. (2018). Gelatin-polysaccharide composite scaffolds for 3D cell culture and tissue engineering: Towards natural therapeutics. Bioengineering Translational Medicine, 4(1), 96–115.
[25] Lopes, C. C. A., Limirio, P. H. J. O, Novais, V. R., & Dechichi, P. (2018). Fourier transform infrared spectroscopy (FTIR) application chemical characterization of enamel, dentin, and bone. Applied Spectroscopy Reviews, 53(9), 747–769.
[26] Gritsch, L., Maqbool, M., Mourino, V., Ciraldo, F. E., Cresswell, M., & Jackson, P. R. (2019). Chitosan/hydroxyapatite composite bone tissue engineering scaffolds with dual and decoupled therapeutic ion delivery: Copper and strontium. Journal of Material Chemistry B, 7(40), 6109–6124.
[27] Milla, L. E., Indrani, D. J., & Irawan, B. (2018). Sintesis dan uji porositas scaffold hidroksiapatit/alginat. ODONTO Dental Journal, 5(1), 49–53.
[28] Darus, F, & Jaafar, M. (2020). Enhancement of carbonate apatite scaffold properties with surface treatment and alginate and gelatine coating. Journal of Porous Materials, 27(3), 831–842.
[29] Abbasi, N., Hamlet, S., Love, R. M., & Nguyen, N. T. (2020). Porous scaffolds for bone regeneration. Journal of Science: Advanced Materials and Devices, 5(1), 1–9.
[30] Lu, J., Yu, H., & Chen, C. (2017). Biological properties of calcium phosphate biomaterials for bone repair: A review. RSC Advances, 8(4), 2015–2033.
[31] Hayashi, K., Kishida, R., Tsuchiya, A., Ishikawa, K., Kishida, R., & Tsuchiya, A. (2019). Honeycomb blocks composed of carbonate apatite, β-tricalcium phosphate, and hydroxyapatite for bone regeneration: Effects of composition on biological responses. Materials Today Bio, 4(100031), 1–11.
[32] Ebnesajjad, S. (2011). Surface and material characterization techniques. In Handbook of Adhesives and Surface Preparation. 31–48.
[33] Mohd, P. N. A. S., Koshy, P., Abdullah, H. Z., Idris, M. I., & Lee, T. C. (2019). Syntheses of hydroxyapatite from natural sources. Heliyon, 5(5), 1–14.
[34] Jeong, J., Kim, J. H., Shim, J. H., Hwang, N. S., & Heo, C. Y. (2019). Bioactive calcium phosphate materials and applications in bone regeneration. Biomaterial Resolution, 23(1), 1–11.
[35] Ana, I. D., Matsuya, S., & Ishikawa, K. (2010). Engineering of carbonate apatite bone substitute based on composition-transformation of gypsum and calcium hydroxide. Engineering. 2(5), 344–352.
[36] Peter, M., Ganesh, N., Selvamurugan, N., Nair, S. V., Furuike, T., & Tamura, H. (2010). Preparation and characterization of chitosan-gelatin/nanohydroxyapatite composite scaffolds for tissue engineering applications. Carbohydrate Polymer, 80(3), 687–694.
[37] Zhou, H., & Lee, J. (2011). Nanoscale hydroxyapatite particles for bone tissue engineering. Acta Biomaterialia, 7(7), 2769-2781.
[38] Ari, M. D. A., Yuliati, A., Rahayu, R. P., & Saraswati, D. (2018). The differences scaffold composition in pore size and hydrophobicity properties as bone regeneration biomaterial. Journal of International Dental and Medical Research, 11(1), 318-322.
[39] El-Hefian, E. A., Nasef, M. M., & Yahaya, A. H. (2014). Chitosan-based polymer blends: Current status and applications. Journal Chemical Society of Pakistan, 36(1), 11–27.
[40] Zhang, N., Liu, H., Yu, L., Liu, X., Zhang, L., Chen, L. & Shanks, R. (2013). Developing gelatin–starch blends for use as capsule materials. Carbohydrate Polymers, 92(1), 455–461.
[41] Cao, H., Chen, M. M., Liu, Y., Liu, Y. Y., Huang, Y. Q., Wang, J. H., Chen, J. D. & Zhang, Q. Q. (2015). Fish collagen-based scaffold containing PLGA microspheres for controlled growth factor delivery in skin tissue engineering. Colloids and Surfaces B: Biointerfaces, 136, 1098–1106.
[42] Lee, J. & Yun, H. S. (2014). Hydroxyapatite-containing gelatin/chitosan microspheres for controlled release of lysozyme and enhanced cytocompatibility. Journal of Materials Chemistry B, 2(9), 1255–1263.
[43] Ghorbani, M. & Roshangar, L. (2019). Construction of collagen/nanocrystalline cellulose based-hydrogel scaffolds: synthesis, characterization, and mechanical properties evaluation. International Journal of Polymeric Materials and Polymeric Biomaterials, 1–7.
[44] Liu, Y., Gu, Y., & Fan, D. (2020). Fabrication of high-strength and porous hybrid scaffolds based on nano-hydroxyapatite and human-like collagen for bone tissue regeneration. Polymers (Basel), 12(61), 1– 17.

The Characteristics, Swelling Ratio and Water Content Percentage of Chitosan-gelatin/limestone-based Carbonate Hydroxyapatite Composite Scaffold

ORIGINALITY REPORT

18%	13%	13%	1%
SIMILARITY INDEX	INTERNET SOURCES	PUBLICATIONS	STUDENT PAPERS

PRIMARY SOURCES

1	eprints.utm.my Internet Source	2%
2	www.jidmr.com Internet Source	2%
3	Submitted to Universitas Airlangga Student Paper	1%
4	www.csir.org.gh Internet Source	1%
5	pure.coventry.ac.uk Internet Source	1%
6	Peter, M.. "Preparation and characterization of chitosan@?gelatin/nanohydroxyapatite composite scaffolds for tissue engineering applications", Carbohydrate Polymers, 20100505 Publication	<1%
7	www.ejurnal-analiskesehatan.web.id Internet Source	<1%

8	Mohamed S. Draz, Anish Vasan, Aradana Muthupandian, Manoj Kumar Kanakasabapathy et al. "Virus detection using nanoparticles and deep neural network–enabled smartphone system", Science Advances, 2020 Publication	<1 %
9	rjptonline.org Internet Source	<1 %
10	Asep Handaya Saputra, Rizky Adi Purwoko. "Swelling properties of CMC-based hydrogel from water hyacinth with piper betel leaves extract addition", AIP Publishing, 2018 Publication	<1 %
11	us-central1-dental-press.cloudfunctions.net Internet Source	<1 %
12	www.nature.com Internet Source	<1 %
13	"Polymeric and Natural Composites", Springer Science and Business Media LLC, 2022 Publication	<1 %
14	ejournal3.undip.ac.id Internet Source	<1 %
15	repo.uum.edu.my Internet Source	<1 %
16	uatscimath.ipst.ac.th	

	Internet Source	<1%
17	www.coursehero.com Internet Source	<1%
18	www.frontiersin.org Internet Source	<1%
19	"Design and Applications of Hydroxyapatite - Based Catalysts", Wiley, 2022 Publication	<1%
20	"Sustainable Agriculture Reviews 36", Springer Science and Business Media LLC, 2019 Publication	<1%
21	Zahrah Hikmah, Anang Endaryanto, I. Dewa Gede Ugrasena, Anny Setijo Rahaju, Syaiful Arifin. "Nigella sativa L. as immunomodulator and preventive effect on renal tissue damage of lupus mice induced by pristane", Heliyon, 2022 Publication	<1%
22	link.springer.com Internet Source	<1%
23	epa.gov Internet Source	<1%
24	mdpi.com Internet Source	<1%

25	repository.up.ac.za Internet Source	<1 %
26	"Innovative Bioceramics in Translational Medicine I", Springer Science and Business Media LLC, 2022 Publication	<1 %
27	Mareeswari Paramasivan, T. S. Sampath Kumar, Hemalatha Kanniyappan, Vignesh Muthuvijayan, T. S. Chandra. "Biomimetic ion substituted and Co-substituted hydroxyapatite nanoparticle synthesis using Serratia Marcescens", Scientific Reports, 2023 Publication	<1 %
28	iopscience.iop.org Internet Source	<1 %
29	journals.sagepub.com Internet Source	<1 %
30	pji.ub.ac.id Internet Source	<1 %
31	Jihang Yao, Zhewen Liu, Wendi Ma, Wenying Dong, Yilong Wang, Haibo Zhang, Mei Zhang, Da-Hui Sun. "Three-dimensional coating of SF/PLGA coaxial nanofiber membranes on surfaces of calcium phosphate cement for enhanced bone regeneration", ACS Biomaterials Science & Engineering, 2020 Publication	<1 %

32	K.C. Vinoth Kumar, T. Jani Subha, K.G. Ahila, B. Ravindran, S.W. Chang, Ahmed Hossam Mahmoud, Osama B. Mohammed, M.A. Rathi. "Spectral characterization of hydroxyapatite extracted from Black Sumatra and Fighting cock bone samples: A comparative analysis", Saudi Journal of Biological Sciences, 2020 Publication	<1 %
33	Maria Apriliani Gani, Aniek Setiya Budiatin, Dewi Wara Shinta, Chrismawan Ardianto, Junaidi Khotib. "Bovine hydroxyapatite-based scaffold accelerated the inflammatory phase and bone growth in rats with bone defect", Journal of Applied Biomaterials & Functional Materials, 2023 Publication	<1 %
34	Pawan Kumar, Brijnandan S. Dehiya, Anil Sindhu, Ravinder Kumar, Catalin I. Pruncu, Anil Yadav. "Fabrication and characterization of silver nanorods incorporated calcium silicate scaffold using polymeric sponge replica technique", Materials & Design, 2020 Publication	<1 %
35	Sara Pourshahrestani, Ehsan Zeimaran, Nahrizul Adib Kadri, Nicola Gargiulo et al. "Potency and Cytotoxicity of a Novel Gallium-Containing Mesoporous Bioactive Glass/Chitosan Composite Scaffold as	<1 %

Hemostatic Agents", ACS Applied Materials & Interfaces, 2017
Publication

36	etheses.whiterose.ac.uk Internet Source	<1 %
37	garuda.kemdikbud.go.id Internet Source	<1 %
38	westminsterresearch.westminster.ac.uk Internet Source	<1 %
39	www.amrita.edu Internet Source	<1 %
40	www.science.gov Internet Source	<1 %
41	"Innovative Bioceramics in Translational Medicine II", Springer Science and Business Media LLC, 2022 Publication	<1 %
42	Abdul Halim Daulay, Decky Jusiana Indrani, Muhammad Rifqi Aufan, Aditianto Ramelan et al. "Bone Scaffold Based on Biopolymer/Carbonate Apatite by Freeze Drying Method: Synthesis, Characterization, and *In Vitro* Cytotoxicity", Materials Science Forum, 2015 Publication	<1 %

43	Ahmed Madni, Rozina Kousar, Naveera Naeem, Fazli Wahid. "Recent Advancements in Applications of Chitosan-based Biomaterials for Skin Tissue Engineering", Journal of Bioresources and Bioproducts, 2021 Publication	<1 %
44	Alexander Laskin, Martin J. Iedema, James P. Cowin. "Time-Resolved Aerosol Collector for CCSEM/EDX Single-Particle Analysis", Aerosol Science and Technology, 2003 Publication	<1 %
45	Doan Van Hong Thien, Ming Hua Ho, Sheng Wen Hsiao, Chung Hsing Li. "Wet chemical process to enhance osteoconductivity of electrospun chitosan nanofibers", Journal of Materials Science, 2014 Publication	<1 %
46	Jing Xiang, Yuzhou Li, Mingxing Ren, Ping He, Fengyi Liu, Zheng Jing, Yong Li, He Zhang, Ping Ji, Sheng Yang. "Sandwich-like nanocomposite electrospun silk fibroin membrane to promote osteogenesis and antibacterial activities", Applied Materials Today, 2022 Publication	<1 %
47	Paula I.P. Soares, Joana Romão, Ricardo Matos, Jorge Carvalho Silva, João Paulo Borges. "Design and engineering of magneto-responsive devices for cancer theranostics:	<1 %

nano to macro perspective", Progress in Materials Science, 2020
Publication

48	Sonja Kuth, Liliana Liverani. "Biodegradable and bioactive polymer/inorganic phase composites", Elsevier BV, 2022 Publication	<1 %
49	Wenxue Sun, Yaohan Zhang, Le Jia. "Polysaccharides from Agrocybe cylindracea residue alleviate type 2-diabetes-induced liver and colon injuries by p38 MAPK signaling pathway", Food Bioscience, 2022 Publication	<1 %
50	core.ac.uk Internet Source	<1 %
51	dokumen.pub Internet Source	<1 %
52	eventclass.org Internet Source	<1 %
53	ijdm.co.in Internet Source	<1 %
54	mdpi-res.com Internet Source	<1 %
55	repository.nwu.ac.za Internet Source	<1 %

www.pertanika.upm.edu.my

56	Internet Source	<1%
57	"Biomaterials in Tissue Engineering and Regenerative Medicine", Springer Science and Business Media LLC, 2021 Publication	<1%
58	Arvelakis, S.. "Agglomeration problems during fluidized bed gasification of olive-oil residue: evaluation of fractionation and leaching as pre-treatments^*", Fuel, 200307 Publication	<1%
59	Hanan H. Beherei. "Preparation, Bioactivity and Antibacterial Effect of Bioactive Glass/Chitosan Biocomposites", IFMBE Proceedings, 2009 Publication	<1%
60	Nura Brimo, Dilek Çökeliler Serdaroğlu, Tansel Uyar, Busra Uysal, Elif Bahar Çakıcı, Miris Dikmen, Zerrin Canturk. "Novel Electrospun Polymeric Nanofibers Loaded Different Medicaments as Drug Delivery Systems for Regenerative Endodontics", Current Drug Delivery, 2023 Publication	<1%
61	"Engineering Materials for Stem Cell Regeneration", Springer Science and Business Media LLC, 2021 Publication	<1%

Exclude quotes	Off	Exclude matches	Off
Exclude bibliography	On		

The Characteristics, Swelling Ratio and Water Content Percentage of Chitosan-gelatin/limestone-based Carbonate Hydroxyapatite Composite Scaffold

GRADEMARK REPORT

FINAL GRADE

/0

GENERAL COMMENTS

Instructor

PAGE 1

PAGE 2

PAGE 3

PAGE 4

PAGE 5

PAGE 6

PAGE 7

PAGE 8

PAGE 9

PAGE 10

PAGE 11